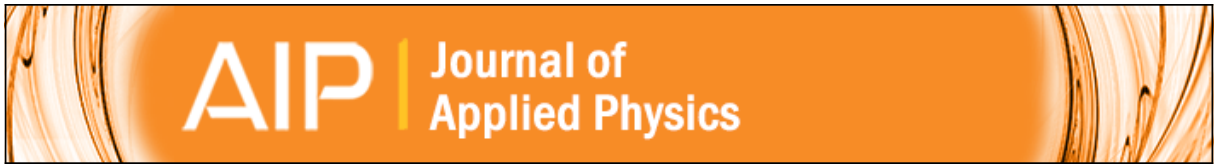

Effect of Nb-donor and Fe-acceptor dopants in (Bi 1 / 2 Na 1 / 2) TiO 3 – BaTiO 3 – (K 0.5 Na 0.5) NbO 3 lead-free piezoceramics

Wook Jo, Emre Erdem, Rüdiger-A. Eichel, Julia Glaum, Torsten Granzow, Dragan Damjanovic, and Jürgen Rödel

Citation: Journal of Applied Physics **108**, 014110 (2010); doi: 10.1063/1.3437645

View online: http://dx.doi.org/10.1063/1.3437645

View Table of Contents: http://scitation.aip.org/content/aip/journal/jap/108/1?ver=pdfcov

Published by the AIP Publishing

Effect of Nb-donor and Fe-acceptor dopants in $(Bi_{1/2}Na_{1/2})TiO_3-BaTiO_3-(K_{0.5}Na_{0.5})NbO_3$ lead-free piezoceramics

Wook Jo,[1,a)] Emre Erdem,[2] Rüdiger-A. Eichel,[2] Julia Glaum,[1] Torsten Granzow,[1] Dragan Damjanovic,[3] and Jürgen Rödel[1]
[1]*Institute of Materials Science, Technische Universität Darmstadt, Petersenstrasse 23, 64287 Darmstadt, Germany*
[2]*Institut für Physikalische Chemie, Albert-Ludwigs-Universität Freiburg, Albertstrasse 21, 79104 Freiburg, Germany*
[3]*Ceramics Laboratory, Swiss Federal Institute of Technology, EPFL, Lausanne CH-1015, Switzerland*

(Received 5 March 2010; accepted 5 May 2010; published online 13 July 2010)

The role of Fe as an acceptor and Nb as a donor in $[0.94-x](Bi_{1/2}Na_{1/2})TiO_3-0.06BaTiO_3-x(K_{0.5}Na_{0.5})NbO_3$ (100xKNN) (x=0.02 and 0.03) lead-free piezoceramics was investigated. X-ray diffraction analyses show that all the profiles are best-fitted with a cubic symmetry where Fe doping tends to induce a lattice expansion, while Nb doping does the opposite. The strain and polarization characteristics are enhanced and suppressed by the acceptor and donor dopants, respectively. The improvement in the electrical properties with acceptor doping is accompanied by the stabilization of a ferroelectric order. Electron paramagnetic resonance spectroscopic analysis suggests that the stabilization of the ferroelectric order by the Fe dopant originates from the formation of $(Fe'_{Ti}-V_O^{\bullet\bullet})^{\bullet}$ defect dipoles. © *2010 American Institute of Physics*. [doi:10.1063/1.3437645]

I. INTRODUCTION

Piezoelectric materials are characterized by their ability to convert mechanical stress into an electric polarization or an electric field into a mechanical strain. This property has led to their employment in a wide range of sensing and actuating systems.[1] Ferroelectric materials with the perovskite structure are among the best piezoelectric materials available; in particular, solid solutions such as lead zirconate titanate ($Pb[Zr_xTi_{1-x}]O_3$, PZT), especially for the compositions around the morphotropic phase boundary (MPB) at x=0.525, or lead magnesium niobate–lead titanate ($Pb[Mg_{2/3}Nb_{1/3}]O_3-PbTiO_3$, PMN–PT) have found widespread use since the 1960s.[2] More recently, a large effort has been made to develop lead-free alternatives to existing lead-containing piezoelectrics, instigated in large part by legislation around the globe to limit the use of toxic heavy metals such as lead.[3] Many of these investigations have focused on materials based on Bi-containing solid solutions, such as $[Bi_{1/2}Na_{1/2}]TiO_3-BaTiO_3$ (BNT–BT).[3,4] This system is particularly interesting since the electronic structure of Bi^{3+} is similar to that of Pb^{2+}, and at ambient temperature the existence of an MPB between rhombohedral BNT and tetragonal BT has been reported in the BNT–BT system for BT-contents of around 6%–7%.[3] A second system that has received much attention is $[K_{0.5}Na_{0.5}]NbO_3$ (KNN),[3,5] although the phase boundary in this system was eventually shown to be a polymorphic phase boundary instead of an MPB.[3,6]

One reason for the versatility of PZT is the possibility to fine-tune its properties by doping with different elements. In the literature there are comparably few reports on the isovalent doping of PZT (Refs. 7 and 8); according to Berlincourt,[9] it has little influence on the material parameters except for a decrease in the Curie temperature and an increase in the permittivity. The effects are more pronounced when doping with donor ions; typical donors in PZT are La^{3+} or Bi^{3+}, replacing Pb^{2+} on the A site, and Nb^{5+} or Sb^{5+}, substituting for Ti^{4+} or Zr^{4+} on the B-site.[9] Donor-doping generally leads to a destabilization of the ferroelectric domain structure, resulting in a decrease in the Curie temperature and ferroelectric coercive field but an increase in permittivity, piezoelectric coupling, and mechanical compliance. Donor doped materials are also referred to as "soft," an attribute that can refer both to the electrical and the mechanical properties.

Typical acceptor doping ions in PZT are K^+ or Na^+ on the A site and Fe^{3+} on the B site. Their effect is opposite to that of donors such as: they stabilize the domain structure[10–13] and are, therefore, often referred to as "hard" dopants. They also tend to promote pronounced "aging" features, e.g., the change in permittivity with time.[14] Aging also changes the shape of the ferroelectric hysteresis;[15] it was proposed that aging be due to an internal bias field that stabilizes the domain configuration.[16,17] There are two competing models for explaining these effects. One is based on defect associates of doping ions and oxygen vacancies that have been evidenced in acceptor-doped systems.[18–21] These defect dipoles, referred to as "symmetry conforming defects" by Ren and co-workers,[22–24] reduce the domain wall mobility and stabilize the present domain structure by imposing their symmetry on the surrounding domains.[16,25] The second model for explaining the aging effect is based on the existence of charge carriers that can move over distances of more than one unit cell. Acceptor doping generally increases the number of free charge carriers present. The charge carriers are redistributed during aging; the driving force is generally

[a)]Author to whom correspondence should be addressed. Electronic mail: jo@ceramics.tu-darmstadt.de.

considered to be related to depolarization fields at domain walls, at grain boundaries,[26–28] inside the grains,[15] or at the sample surface.[25] Because even a slight redistribution of charge carriers is sufficient to compensate these depolarizing fields,[29] the charges accumulating at domain walls will effectively hinder domain wall motion.[27,28]

Donor doping and acceptor doping obviously have a profound effect on domain stability in systems like PZT. Still, their effect on BNT-based lead-free materials has not been systematically studied in detail, though there are a couple of reports for the effect of defect-generating dopants on depolarization temperature T_d.[30,31] This is surprising when one considers that the stability of ferroelectric domain structures is of paramount relevance for the performance of these systems. BNT–BT exhibits a T_d and a transition into a nonparaelectric high-temperature phase. Depending on composition, T_d can be as low as 100 °C.[32] An earlier publication designated the high-temperature phase as antiferroelectric,[4] but more recent studies cast some doubts on this designation.[32] T_d can be lowered by adding KNN to BNT–BT (Ref. 33); the high-field strain output is usually optimized in the vicinity of T_d. The high strain output was first assigned to an assumed volume change during a field-induced transition from an antiferroelectric to a ferroelectric phase.[33–35] A recent study, however, suggests that it is actually due to a decrease in the stability of the ferroelectric domain structure:[36] if the domain structure is stable, much of the accessible strain is "wasted" by the creation of a remanent strain change; therefore, only a small fraction is available during repeating unipolar cycles. If the domain structure, induced by an external field, is less stable, the total accessible strain hardly changes but the remanent strain drops sharply. As a result, more strain can be induced by an external field during unipolar cycling. It is, therefore, essential to know if and how the domain stability can be adjusted by doping.

In the present investigation, we compare the effects of donor doping and acceptor doping on the electrical and electromechanical properties of BNT–BT–KNN. A possible stabilizing effect on domain wall structure will be discussed in comparison to the effect of similar doping materials on PZT.

II. EXPERIMENTAL PROCEDURE

$[0.94-x](Bi_{1/2}Na_{1/2})TiO_3-0.06BaTiO_3-x(K_{0.5}Na_{0.5})NbO_3$ (100xKNN) (x=0.02 and 0.03) as matrix materials and their doped derivatives were prepared using the conventional solid oxide route with elemental reagent grade oxides and carbonates. For the doped derivatives, both 1 at. % of Fe^{3+} as an acceptor (referred hereafter to A_100xKNN) and 1 at. % of Nb^{5+} as a donor (D_100xKNN) were substituted for Ti. Partly due to the small amount of substitution level and due to a rather high complexity in A-site constituents, the formation of possible cation vacancies by Nb doping was not taken into account for the stoichiometric formula. All the weighed powders submerged in ethanol were ball-milled in a planetary mill (Frisch) using yttria stabilized zirconia balls for 24 h. Sieved and dried powders were calcined in a covered alumina crucible at 900 °C for 3 h. To refine the particle size as well as to crush agglomerates, the calcined powders were ground and again ball-milled in a planetary mill for 24 h. The obtained powders of each composition were uniaxially compacted into pellets and pressed hydrostatically at 300 MPa. All the specimens were heated up to 1100 °C at a rate of 5 °C/min, sintered for 3 h, and cooled in the furnace.

Purity and formation of the desired phase were monitored for both calcined and sintered samples by powder X-ray diffraction (XRD, STOE STADIP) using Cu $K\alpha_1$ radiation. The structural simulation was done with FULLPROF software.[37] The details of the chemical homogeneity of the matrix materials, the deviation of which could also create unintended defects due to the volatile elements such as Bi, K, Na, were checked by inductively coupled plasma spectroscopy (ICP, Clariant Produkte GmbH, Germany). The average grain size was determined from the images of scanning electron microscopy (XL 30 FEG, Philips) by a linear intercept method. Strain and polarization hysteresis loops were measured on disk shaped samples, polished, and electroded with silver paint, using a Sawyer–Tower circuit equipped with a linear variable differential transformer (LVDT) displacement sensor attached. A triangular shaped wave form with the field amplitude of 8 kV/mm and the frequency of 50 mHz was used. To monitor volume changes during electric cycling, two additional LVDTs placed perpendicular to the one for axial strain measurements were used.[36] Deaging experiments were performed for the A_2KNN. The samples were electrically cycled with a bipolar, triangular signal at 6 kV/mm. The frequency was chosen to be 55 mHz for the first ten cycles. For higher cycle numbers 100 mHz was used. After each cycling step the polarization was measured in a Sawyer–Tower circuit with a 15 μF measurement capacitance. A bipolar triangular signal with an amplitude of 6 kV/mm and a frequency of 55 mHz was used throughout all the measurements.

In order to characterize the changes in defect structure induced by the addition of Fe, *X*-band (9.46 GHz) electron paramagnetic resonance (EPR) measurements were carried out on a spectrometer (EMX 300E, Bruker) using a rectangular resonator. The magnetic field was read out with a nuclear magnetic resonance gaussmeter (ER 035M, Bruker), and as a standard field marker, polycrystalline 2,2-diphenyl-1-picrylhydrazyl with $g=2.0036$ was used for the exact determination of the resonance magnetic field values and the *g*-factor.

III. RESULTS AND DISCUSSION

Figure 1(a) shows the XRD profiles taken from as-sintered bulk samples of 2KNN, D_2KNN, and A_2KNN ceramics. All the samples display the symmetry related to a typical perovskite structure, and no traceable secondary phase is detected within the resolution limit of the currently used diffractometer. All the diffraction patterns are best-fitted with a cubic $Pm\bar{3}m$. Any deviation from $Pm\bar{3}m$ such as a rhombohedral or a tetragonal or a mixture of both resulted in a relatively large deviation between the observed and simulated profiles. An expanded view on the pseudocubic {111}

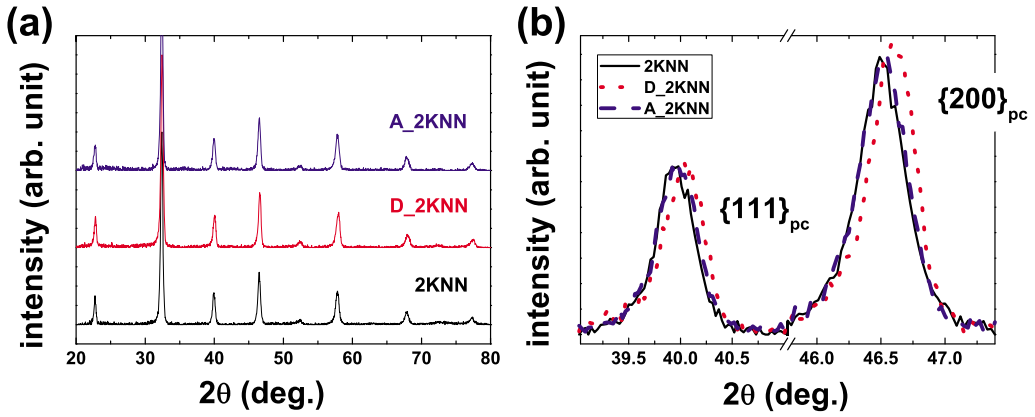

FIG. 1. (Color online) XRD profiles for 2KNN-based piezoceramics. Note that the addition of the acceptor induces practically no change in the XRD profile, while that of the donor leads to a contraction in the lattice parameter.

and {200} peaks presented in Fig. 1(b) again supports the fact that there is no obvious long-range noncubic distortion, which is consistent with our previous observations.[34,38,39] Spreitzer *et al.*[40] showed that the rhombohedral distortion of pure BNT can be significantly suppressed and consequently appear as a cubiclike structure when Na is deficient. To check this possibility that currently observed cubiclike structures could also be due to a notable deficiency in alkaline elements such as Na and K, ICP spectroscopy was conducted on 2KNN. As shown in Table I, no evidence of chemical deviation in the concentration of each element in the sintered specimen from the intended chemistry was detected within the experimental error range, which indicates that the use of atmospheric powder during sintering of the systems investigated effectively suppresses the evaporation of the known volatile elements. It is interesting to notice that the introduction of Nb as a donor induces a lattice contraction, while no visible change in the diffraction profile is detectable in A_2KNN. In spite of the visible difference in the XRD profile between 2KNN and D_2KNN, practically no difference in both Archimedes density (99%) and average grain size (~ 2 μm) was observed. However, a significant deviation in both Archimedes density (97%) and the average grain size (~ 10 μm) was observed in A_2KNN.

To facilitate further discussion of the dopant effects, it is convenient to introduce two parameters that best-characterize the ferroelectric stability of the materials studied. Figures 2(a) and 2(b) provide the employed electrical signal with various offset fields and resulting unipolar strain hysteresis of 2KNN, respectively. It is seen that both longitudinal (S_{33}) and radial strain (S_{11}) of 2KNN show a quadratic increase up to about 5 kV/mm. Above 5 kV/mm, they increase rather sharply until they start saturating at about 6 kV/mm. Based on the phenomenological similarity with the poling strain curves of usual ferroelectric materials, the inflection point located at about 5.6 kV/mm is now referred to as poling field (E_{pol}) where a major portion of switchable ferroelectric domains aligns along the applied electric field direction.[36,41]

In the meantime, it should be noted that below E_{pol}, even the volume change increases quadratically. This indicates that the dominating strain mechanism below E_{pol} is merely electrostrictive,[36,42,43] which does not require switchable ferroelectric domains. Considering the pseudocubic symmetry at its unpoled state as well as the fact that non-180° domain switching is only a function of deviatoric strain that is volume-conserving, it is expected that the ferroelectric domains in this system, whose presence is evident from the existing large hysteresis above E_{pol}, would appear only under the application of electric field. In fact, this is consistent with our previous observations that freshly sintered samples are free of ferroelectric domains,[34] and they are only observable on the application of a certain amount of electric field.[42] On the other hand, it should also be noted that the induced poled state of the currently investigated material is not stable enough to induce a remanent strain on the removal of the electric field and is disrupted completely at zero field. It was proposed that this absence of remanent strain possibly caused by a destabilization of electric-field-induced ferroelectric order at zero field be the origin of the large actuating performance featured by the large signal d_{33} of ~ 550 pm/V.[36] Thereby, it is very useful to introduce a parameter that can best-characterize the stability of ferroelectric order. One such parameter, which will be referred to as a "depoling" field (E_{dep}) throughout the context, is the electric field value where a significant back-switching of field-induced ferroelectric domains happens. This field is determined at the inflection point in the strain versus electric field

TABLE I. Comparison of the concentration of each element in 2KNN between the intended and ICP-determined values (all in mol %).

	Bi	Na	K	Nb	Ba	Ti
Intended	0.46	0.47	0.01	0.02	0.06	0.98
Measured	0.47	0.48	0.0118	0.0194	0.063	0.95
Accuracy	0.01	0.01	0.0004	0.0006	0.002	0.03

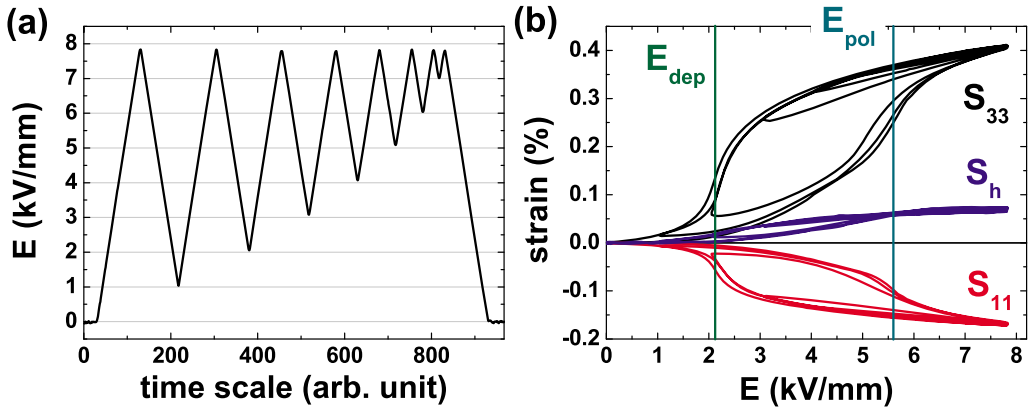

FIG. 2. (Color online) (a) unipolar strain hysteresis along (S_{33}) and perpendicular to (S_{11}) the electric field as well as a concurrent volume change (S_h) with the multiple of 1 kV/mm offset fields (b) electric field profile used for the strain measurement in (a).

curve to avoid any possible arbitrariness in determination. In the case of 2KNN E_{dep} has been determined as 2.1 kV/mm.

Bipolar strain and polarization hysteresis loops of 2KNN, D_2KNN, and A_2KNN are displayed in Figs. 3(a) and 3(b), respectively. Compared with 2KNN, a significant decrease in E_{pol} (~4.6 kV/mm) and E_{dep} (not existing) is observed in A_2KNN, which indicates a ferroelectric order is both easier to be induced and more stable against the removal of the field. Together with the increase in the remanent polarization (P_{rem}) and the development of S_{neg} in A_2KNN, it can be said that the role of the acceptor is increasing the stability of poling-induced ferroelectric order, since P_{rem} and S_{neg} are the measures that a certain degree of poling-induced domain structure remains on removal of the electric field.[36] In the meantime, a relative increase in E_{pol} (~6.5 kV/mm) and E_{dep} (~2.7 kV/mm) in D_2KNN implies the role of donor is to unfavor the ferroelectric order, although the effect is not quite pronounced in the presented hysteresis loops in terms of P_{rem} and S_{neg}.

Figure 4(a) provides the diffraction profiles of 3KNN, D_3KNN, and A_3KNN for a selected angular range highlighting $\{111\}_{pc}$ and $\{200\}_{pc}$ peaks in comparison to that of 2KNN. In contrast to the 2KNN-based systems, a notable effect of doping is only visible in the A_3KNN system, e.g., lattice expansion by acceptor doping. Together with the diffraction study of the 2KNN-based systems, it can be said that Fe as an acceptor and Nb as a donor induce a lattice expansion and contraction, respectively. On the other hand, it is interesting to note that the introduction of additional 1 mol % KNN to 2KNN leads to a practically similar effect to that of Nb addition, suggesting that the role of KNN itself appears to resemble that of a donor. Indeed, it is seen that there exist phenomenological similarities between the role of KNN and Nb as shown in Fig. 4(b). It shows that the strain hysteresis curve of 3KNN-based materials is comparable to that of 2KNN. The degree of depression in the total strain level and the change in E_{pol} (~6.9 kV/mm) and E_{dep} (2.8 kV/mm) are in a good agreement with those of D_2KNN (see Table II). Besides, the effect of acceptor and donor doping is, respectively, less and more pronounced for 3KNN than for 2KNN systems.

In order to provide further insight into the impact of acceptor doping on the defect structure of the 2KNN system, EPR spectroscopy was applied.[44] The EPR spectrum of A_2KNN as compared to 2KNN is depicted in Fig. 5(a). The spectrum for 2KNN shows resonances only in the $g=2.0-1.9$ region owing to defects in a comparatively small concentration. In order to identify these in more detail, a spectrum with an enhanced resolution, as shown in Fig. 5(b), was recorded. The corresponding resonances may be explained in terms either of Ti'_{Ti}, Nb'_{Nb}, and O'_O defect centers, all of which act as acceptors or of a singly charged oxygen va-

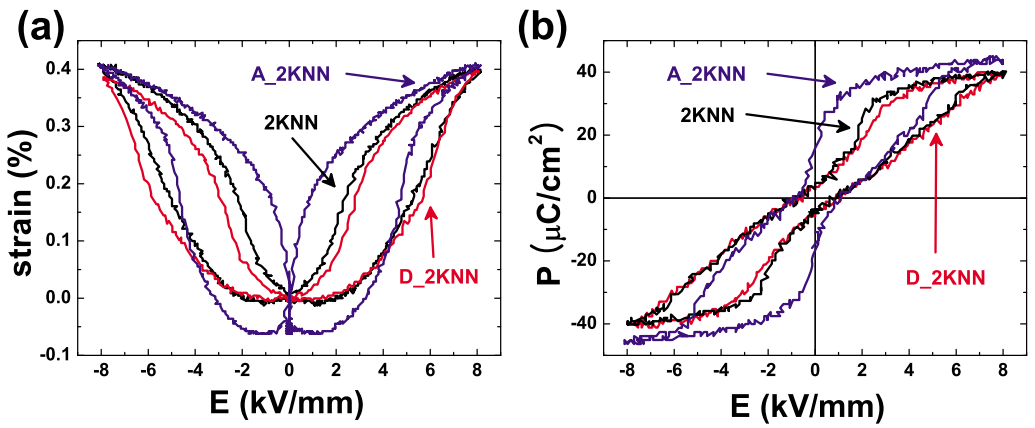

FIG. 3. (Color online) (a) bipolar strain and (b) polarization hysteresis loops of 2KNN, D_2KNN, and A_2KNN.

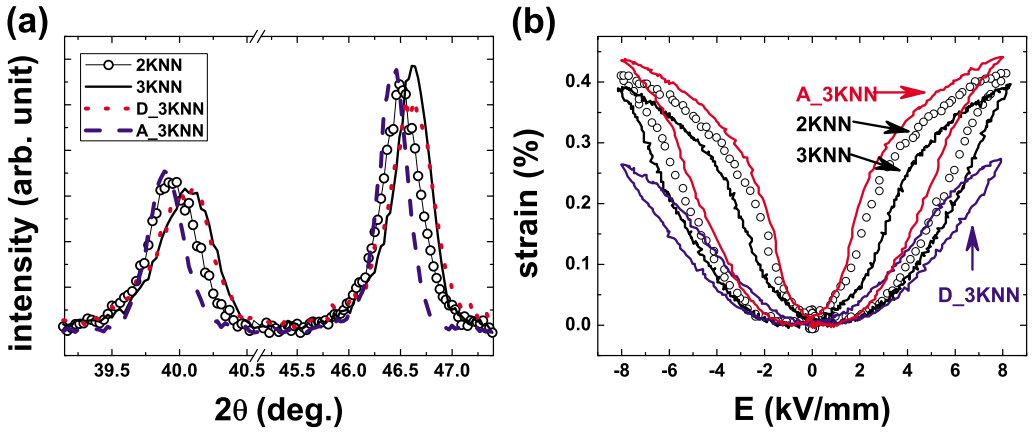

FIG. 4. (Color online) (a) XRD profiles and bipolar strain hysteresis loops of 3KNN, D_3KNN, and A_3KNN in comparison with that of 2KNN.

cancy ($V_O^{\bullet}$) that acts as donor. For a definite assignment, a further systematic investigation is needed. Because the concentration of these defects is rather small, and as all of these defects disappear after acceptor doping, we did not dwell on this any further. On the other hand, the EPR spectrum of A_2KNN shows strong signals in the low-field region, i.e., 100 mT, 170 mT and a broad resonance at $g=2.0$ (350 mT). The former is characteristic for Fe^{3+} incorporated in the octahedrally-coordinated perovskite B-site, forming a $(Fe'_{Ti}-V_O^{\bullet\bullet})^{\bullet}$ defect dipole for partial charge compensation.[45] This suggests that the stabilization of the ferroelectric order with Fe dopants is closely related to the formation of this defect dipole. Note that these defect dipoles are often discussed as being responsible for a "*hardening*" of Fe-doped PZT,[16,46] even though they also appear in *soft* codoped PZT.[47]

The resonance at $g=2.0$ is assigned to "free" Fe cations, i.e., Fe'_{Ti} functional centers not associated with an oxygen vacancy. The observed signal can be distinguished from that of a magnetically active secondary phase by means of the EPR line-width,[48] which is considerably broader for an exchange-coupled magnetic phase. By numerical double-integration of the EPR spectra as well as in comparison with a sample of known spin concentration, it is found that the signal for the $(Fe'_{Ti}-V_O^{\bullet\bullet})^{\bullet}$ defect dipole has approximately the same intensity as that for the free Fe centers. This leads to the conclusion that the two defect centers mutually compensate each other and thereby the overall mechanism for charge compensation in A_2KNN can be written as

$$3[V'''_{Bi}]+2[V''_{Ba}]+[V'_{Na}]+[V'_{K}]+[Fe'_{Ti}]\approx[(Fe'_{Ti}-V_O^{\bullet\bullet})^{\bullet}]+2[V_O^{\bullet\bullet}]$$

The presence of $(Fe'_{Ti}-V_O^{\bullet\bullet})^{\bullet}$ defect dipoles is often proposed as being responsible for the pronounced aging in Fe-doped PZT.[16] From the phenomenological similarity between Fe-doped PZT and A_2KNN in terms of the severely pinched feature in the polarization hysteresis, we attempted to see if the pinched feature disappears by electrically-cycling the specimen in a bipolar mode. No visible difference between the polarization hysteresis of the fresh sample and that of the specimen bipolar-cycled at 100 mHz up to 100 cycles, where all the tested samples broke down, was discerned. This implies that the $(Fe'_{Ti}-V_O^{\bullet\bullet})^{\bullet}$ defect dipoles may not have a noticeable effect on the aging process in the currently investigated systems, possibly due to the difference in the host crystal structures between PZT and 2KNN systems. Whereas in PZT different orientations of the $(Fe'_{Ti}-V_O^{\bullet\bullet})^{\bullet}$ defect dipole within a given PZT unit cell (rhombohedral or tetragonal) involve considerably different potential energies, this is no longer the case for the pseudocubic 2KNN solid solutions. Consequently, the energy needed for defect-dipole reorientation could be markedly lower as compared to PZT.

IV. CONCLUSION

The effect and role of acceptor and donor doping in BNT–BT–KNN systems on the ferroelectric and piezoelectric properties were investigated. It was shown that the donor Nb unfavors the ferroelectric order, which leads to a decrease in the polarization and strain responses, while the acceptor Fe promotes ferroelectric stability with a concurrent increase in both polarization and strain responses. Based on the EPR spectroscopic analysis, it was proposed that the enhanced ferroelectric order in the acceptor-doped system is due to the formation of $(Fe'_{Ti}-V_O^{\bullet\bullet})^{\bullet}$ defect dipoles. Interestingly, no significant hardening or aging was observed in the currently studied BNT–BT–KNN systems. It was suggested that the less pronounced hardening effect of $(Fe'_{Ti}-V_O^{\bullet\bullet})^{\bullet}$ defect dipoles in BNT–BT–KNN systems as compared to PZT may

TABLE II. Summary of E_{pol} and E_{dep} estimated from strain hysteresis loops of all the materials investigated. (All values are in kV/mm and N/A stands for "Not Applicable.")

	2KNN	D_2KNN	A_2KNN	3KNN	D_3KNN	A_3KNN
E_{pol}	5.6	6.5	4.6	6.9	>8	5.7
E_{dep}	2.1	2.7	N/A	2.8	4.0	1.5

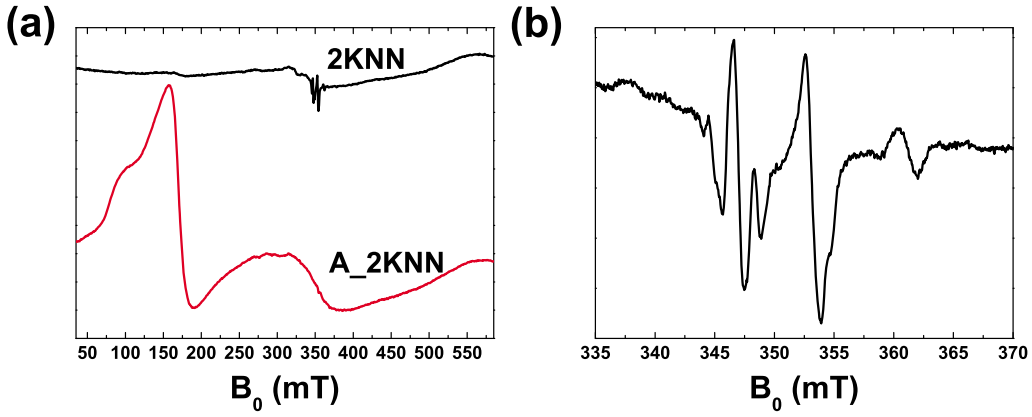

FIG. 5. (Color online) (a) *X*-band (9.46 GHz) EPR spectra of 2KNN and A_2KNN compounds at ambient temperature. (b) Expanded view of the *X*-band (9.46 GHz) EPR spectrum of 2KNN at ambient temperature.

originate from the negligibly small noncubic distortion of BNT–BT–KNN materials, which affords reorientation of the defect dipoles through thermal activation. However, the effect of each dopant is in general quite consistent with that in PZT though the degree of the effect is less pronounced.

ACKNOWLEDGMENT

This work was supported by the Deutsche Forschungsgemeinschaft (DFG) under SFB 595 project.

[1]K. Uchino, *Piezoelectric Actuators and Ultrasonic Motors* (Kluwer Academic, AH Dordrecht, The Netherlands, 1997).
[2]G. H. Haertling, J. Am. Ceram. Soc. **82**, 797 (1999).
[3]J. Rödel, W. Jo, K. T. P. Seifert, E. M. Anton, T. Granzow, and D. Damjanovic, J. Am. Ceram. Soc. **92**, 1153 (2009).
[4]T. Takenaka, K.-I. Maruyama, and K. Sakata, Jpn. J. Appl. Phys., Part 1 **30**, 2236 (1991).
[5]Y. Saito, H. Takao, T. Tani, T. Nonoyama, K. Takatori, T. Homma, T. Nagaya, and M. Nakamura, Nature (London) **432**, 84 (2004).
[6]T. R. Shrout and S. J. Zhang, J. Electroceram. **19**, 113 (2007).
[7]R. Lal, S. C. Sharma, and R. Dayal, Ferroelectrics **100**, 43 (1989).
[8]M. H. Lente, E. N. Moreira, D. Garcia, J. A. Eiras, P. P. Neves, A. C. Doriguetto, V. R. Mastelaro, and Y. P. Mascarenhas, Phys. Rev. B **73**, 054106 (2006).
[9]D. Berlincourt, J. Acoust. Soc. Am. **91**, 3034 (1992).
[10]A. Albareda, R. Pérez, J. E. García, D. A. Ochoa, V. Gomis, and J. A. Eiras, J. Eur. Ceram. Soc. **27**, 4025 (2007).
[11]T. M. Kamel and G. D. With, J. Eur. Ceram. Soc. **28**, 1827 (2008).
[12]M. Morozov, D. Damjanovic, and N. Setter, J. Eur. Ceram. Soc. **25**, 2483 (2005).
[13]M. I. Morozov and D. Damjanovic, J. Appl. Phys. **104**, 034107 (2008).
[14]K. W. Plessner, Proc. Phys. Soc. London, Sect. B **69**, 1261 (1956).
[15]K. Carl and K. H. Härdtl, Ferroelectrics **17**, 473 (1978).
[16]G. Arlt and H. Neumann, Ferroelectrics **87**, 109 (1988).
[17]P. V. Lambeck and G. H. Jonker, J. Phys. Chem. Solids **47**, 453 (1986).
[18]R.-A. Eichel, H. Mestri'c, K.-P. Dinse, A. Ozarowski, J. V. Tol, L. C. Brunel, H. Kungl, and M. J. Hoffmann, Magn. Reson. Chem. **43**, S166 (2005).
[19]V. V. Laguta, Phys. Solid State **40**, 1989 (1998).
[20]H. Meštrić, R.-A. Eichel, K.-P. Dinse, A. Ozarowski, J. v. Tol, and L. C. Brunel, J. Appl. Phys. **96**, 7440 (2004).
[21]W. L. Warren, B. A. Tuttle, F. C. Rong, G. J. Gerardi, and E. H. Poindexter, J. Am. Ceram. Soc. **80**, 680 (1997).
[22]X. Ren, Nature Mater. **3**, 91 (2004).
[23]L. X. Zhang, W. Chen, and X. Ren, Appl. Phys. Lett. **85**, 5658 (2004).
[24]L. X. Zhang and X. Ren, Phys. Rev. B **71**, 174108 (2005).
[25]U. Robels and G. Arlt, J. Appl. Phys. **73**, 3454 (1993).
[26]Y. A. Genenko, J. Glaum, O. Hirsch, H. Kungl, M. J. Hoffmann, and T. Granzow, Phys. Rev. B **80**, 224109 (2009).
[27]M. Takahashi, Jpn. J. Appl. Phys., Part 1 **9**, 1236 (1970).
[28]H. Thomann, Ferroelectrics **4**, 141 (1972).
[29]D. C. Lupascu, Y. A. Genenko, and N. Balke, J. Am. Ceram. Soc. **89**, 224 (2006).
[30]Y. Hiruma, H. Nagata, and T. Takenaka, J. Appl. Phys. **105**, 084112 (2009).
[31]M. Zhu, H. Hu, N. Lei, Y. Hou, and H. Yan, Appl. Phys. Lett. **94**, 182901 (2009).
[32]Y. Hiruma, Y. Watanabe, H. Nagata, and T. Takenaka, Key Eng. Mater. **350**, 93 (2007).
[33]S.-T. Zhang, A. B. Kounga, E. Aulbach, W. Jo, T. Granzow, H. Ehrenberg, and J. Rödel, J. Appl. Phys. **103**, 034108 (2008).
[34]S.-T. Zhang, A. B. Kounga, E. Aulbach, T. Granzow, W. Jo, H.-J. Kleebe, and J. Rödel, J. Appl. Phys. **103**, 034107 (2008).
[35]S.-T. Zhang, A. B. Kounga, E. Aulbach, W. Jo, T. Granzow, H. Ehrenberg, and J. Rödel, Appl. Phys. Lett. **91**, 112906 (2007).
[36]W. Jo, T. Granzow, E. Aulbach, J. Rödel, and D. Damjanovic, J. Appl. Phys. **105**, 094102 (2009).
[37]T. Roisnel and J. Rodriguez-Carvajal, Mater. Sci. Forum **378–381**, 118 (2001).
[38]J. E. Daniels, W. Jo, J. Rödel, V. Honkimäki, and J. L. Jones, Acta Mater. **58**, 2103 (2010).
[39]J. E. Daniels, W. Jo, J. Rödel, and J. L. Jones, Appl. Phys. Lett. **95**, 032904 (2009).
[40]M. Spreitzer, M. Valant, and D. Suvorov, J. Mater. Chem. **17**, 185 (2007).
[41]A. B. Kounga Njiwa, E. Aulbach, T. Granzow, and J. Rödel, Acta Mater. **55**, 675 (2007).
[42]J. Kling, X. Tan, W. Jo, H.-J. Kleebe, H. Fuess, and J. Rödel, J. Am. Ceram. Soc. (to be published).
[43]K. T. P. Seifert, W. Jo, and J. Rödel, J. Am. Ceram. Soc. **93**, 1392 (2010).
[44]R.-A. Eichel, J. Am. Ceram. Soc. **91**, 691 (2008).
[45]H. Meštrić, R.-A. Eichel, T. Kloss, K.-P. Dinse, S. Laubach, S. Laubach, P. C. Schmidt, K. A. Schönau, M. Knapp, and H. Ehrenberg, Phys. Rev. B **71**, 134109 (2005).
[46]P. V. Lambeck and G. H. Jonker, Ferroelectrics **22**, 729 (1978).
[47]E. Erdem, M. D. Drahus, R.-A. Eichel, H. Kungl, M. J. Hoffmann, A. Ozarowski, J. v. Tol, and L. C. Brunel, Funct. Mater. Lett. **1**, 7 (2008).
[48]H.-J. Kleebe, S. Lauterbach, L. Silvestroni, H. Kungl, M. J. Hoffmann, E. Erdem, and R.-A. Eichel, Appl. Phys. Lett. **94**, 142901 (2009).